Canadian Mineralogist
Vol. 30, pp. 771-784 (1992)

PYROCHLORE-GROUP MINERALS IN THE BEAUVOIR PERALUMINOUS LEUCOGRANITE, MASSIF CENTRAL, FRANCE

DANIEL OHNENSTETTER
Centre de Recherche sur la Synthèse et la Chimie des Minéraux, 1a, rue de la Férollerie, 45071 Orléans Cedex 2, France

PATRICE PIANTONE
Bureau de Recherches Géologiques et Minières, B.P. 6009, 45060 Orléans Cedex 2, France

ABSTRACT

Pyrochlore-group minerals are well represented in the upper facies, but virtually absent from the lower facies, in the deep drill-hole from the Beauvoir peraluminous leucogranite, Massif Central, France. These minerals show marked variations in composition, most falling in the microlite subgroup, but some in the pyrochlore subgroup. In addition to the normal isovalent substitution $Ta^{5+} - Nb^{5+}$ at the *B* site, the main substitutions take place at the *A* site and are of complex heterovalent type. In the early uranmicrolite, the substitutions involve U^{4+}, Ca^{2+}, Na^{+} and Sn^{2+} at the *A* site, and F^{-} at the *Y* site. A new substitution scheme is proposed:

$$^{A}[(Na^{+},Ca^{2+})_{2-8/3x}U^{4+}_{x}\square_{5/3\,x}]\ ^{B}[Ta^{5+},\ Nb^{5+})_{2-y}W^{6+}]\ X_6{}^{Y}[(F^{-}_{1+y-z}OH^{-}_{z}),\ O^{2-}_{1-y}]$$

with $x \leq 3/4$. Perturbations in the distribution of cations at the *A* site due to metamictization and hydration of microlite are expressed as a loss of alkalis and fluorine accompanied by an increase in vacancies and the introduction of large-radius cations like K^{+} and Pb^{2+}. This type of transformation in the Beauvoir granite is of the hydrothermal type and may be related to the latest stages of subsolidus interaction between the granite and a meteoric fluid.

Keywords: pyrochlore subgroup, microlite subgroup, peraluminous leucogranite, electron-microprobe data, $U^{4+} - Ca^{2+}$ substitution schemes, metamictization, Beauvoir, France.

SOMMAIRE

Les minéraux du groupe du pyrochlore sont bien représentés dans le faciès supérieur du forage profond réalisé dans le leucogranite hyperalumineux du Beauvoir, dans le Massif Central, (France), et sont pratiquement absents dans le faciès inférieur. Ces minéraux montrent de fortes variations dans leur composition. Ils appartiennent majoritairement au sous-groupe du microlite. Quelques compositions se situent dans le sous-groupe du pyrochlore. Les principales substitutions mises en évidence touchent, outre la classique substitution isovalente $Ta^{5+} - Nb^{5+}$ dans le site *B*, le site *A*. Elles sont de type hétérovalentes complexes. Dans l'uranmicrolite précoce, elles concernent U^{4+}, Ca^{2+}, Na^{+} et Sn^{2+} dans le site *A*, et F^{-} dans le site *Y*. Un schéma de substitution original est proposé:

$$^{A}[(Na^{+},Ca^{2+})_{2-8/3x}U^{4+}_{x}\square_{5/3\,x}]\ ^{B}[Ta^{5+},\ Nb^{5+})_{2-y}W^{6+}]\ X_6{}^{Y}[(F^{-}_{1+y-z}OH^{-}_{z}),\ O^{2-}_{1-y}]$$

avec $x \leq 3/4$. Les perturbations de la distribution des cations dans le site *A* dues à la métamictisation et à l'hydratation du microlite s'expriment par une perte en alcalins et en fluor, et sont accompagnées par une augmentation dans la proportion de lacunes et l'introduction de cations à grand rayon ionique, comme K^{+} et Pb^{2+}. Dans le granite du Beauvoir, ces dernières transformations de type hydrothermal sont à mettre en relation avec les stades ultimes d'interaction entre le granite à l'état subsolidus et une phase fluide météorique.

Mots-clés: sous-groupe du pyrochlore, sous-groupe du microlite, leucogranite hyperalumineux, analyses à la microsonde électronique, schémas de substitutions U^{4+}–Ca^{2+}, métamictisation, Beauvoir, France.

INTRODUCTION

Data on pyrochlore-group minerals present in granitic cupolas are rare and widely dispersed in the literature (Sitnin & Bykova 1962, Kosakevitch 1976); only those from rare-metal-enriched granitic pegmatites (see reviews by Cerny & Ercit 1985, 1989) and carbonatite complexes (see review by Hogarth 1989) have been systematically studied. The deep drill-hole in the Beauvoir albite – lepidolite – topaz leucogranite has made possible a detailed investigation of the crystal chemistry of pyrochlore-group minerals.

The aim of the paper is to show the importance of chemical zoning resulting from the evolution of physicochemical conditions during the crystallization of these minerals. The main substitutions that accompany the

oscillatory zoning are described and modeled. Replacement features and patchy zoning, which correspond to metamictization and hydration, also are described.

Geological Setting

The Echassières granitic complex (Aubert 1969), in the northern Massif Central (Fig. 1), comprises three units: a) the hidden, hypothetical Bosse granite, related to the Bosse ferberite-bearing stockwork, b) the Colettes two-mica leucogranite, and c) the Beauvoir peraluminous leucogranite. They were emplaced during the Early Carboniferous into the Sioule polymetamorphic series (Feybesse & Tegyey 1987). A 900-m-long hole drilled in the context of the "Géologie Profonde de la France" project, intersected an interval of mica schist, the Beauvoir peraluminous leucogranite for more than 700 m to the base of the bore hole, after passing through an interval of alternating schist and sheets of granite. The Beauvoir leucogranite consists of three main facies (Cuney *et al.* 1986). These are, from top to bottom: 1) the B1 facies, about 350 m in apparent thickness, is highly enriched in incompatible elements, as manifested by the presence of lithium- and fluorine-rich minerals such as lepidolite, anhedral primary topaz, fluorite, amblygonite, herderite and microlite. The B1 facies contains abundant primary albite. The B2 facies, about 250 m in apparent thickness, contains first-generation fluorapatite and euhedral quartz and topaz, as well as uraninite. The B3 facies, about 50 m in apparent thickness, contains abundant early K-feldspar and zinnwaldite.

Fig. 1. Location map of the Échassières granite complex showing the limits of the Massif Central in France (stippled).

Facies B1 and B2 have been dated using the Rb/Sr whole-rock method at 299 ± 9 Ma and 312 ± 8 Ma, respectively (Duthou & Pin 1987).

Habit and Distribution of the Pyrochlore-Group Minerals in the Beauvoir Leucogranite

Previous work

Cassiterite and pyrochlore were first reported by Lacroix (1896) in the residues obtained from panning of the Echassières kaolin. Gaspérin (1972) showed unambiguously that the mineral called "néotantalite", found in concentrates by Termier (1902), is in fact microlite with vacancies at the *A* site. Gaspérin (1972) also detected the presence of Ba, Pb, and U, and proposed the replacement of Ca and Na by Ba and Pb in metamictic portions of microlite through the action of hydrothermal solutions.

An exhaustive study of the oxides in cores recovered from the exploratory drill-holes (Kosakevitch 1976) showed that: 1) columbite is the most widespread Nb–Ta mineral, and is associated with tantalite and probable ixiolite, 2) the distribution of elements in the columbite, tantalite and microlite is very complex, and 3) hydration of these phases and leaching of Ca was accompanied by the appearance of Ba and Pb in microlite.

Habit and distribution of microlite throughout the drill-hole

Minerals of the pyrochlore group are rare in facies B2, and euhedral phases completely disappear below 606 m, below which they occur only as relics in columbite–tantalite (Johan *et al.* 1988). They are almost invariably small octahedra with well-developed {111} faces. The crystals vary from 0.1 to 0.8 mm across, and are rarely enclosed in other minerals. The color of the crystals varies with depth, from virtually colorless in the upper part of the Beauvoir granite, to honey-colored greenish yellow at depth. A single crystal may show color variations, from clear yellow in the core to green at the rim. These color variations are due to changes in the chemical composition of the crystals. These different chemical compositions are observed in back-scattered electron (BSE) images (Figs. 2A, 2B). Some crystals have a porous external zone that gives them a milky white appearance, similar to those observed in the preliminary drill-holes (Kosakevitch 1976).

Replacement of the pyrochlore-group minerals by columbite-group minerals seems to be the most common (Fig. 2C), as pointed out by Aubert (1969). This type of replacement is equivalent to pseudomorphism by columbite (James & McKie 1958) and the "columbitization" reaction of Van der Veen (1963), but inverse relationships also exist (Fig. 2D). In this figure, a grain of zoned manganocolumbite is intergrown with microlite, which

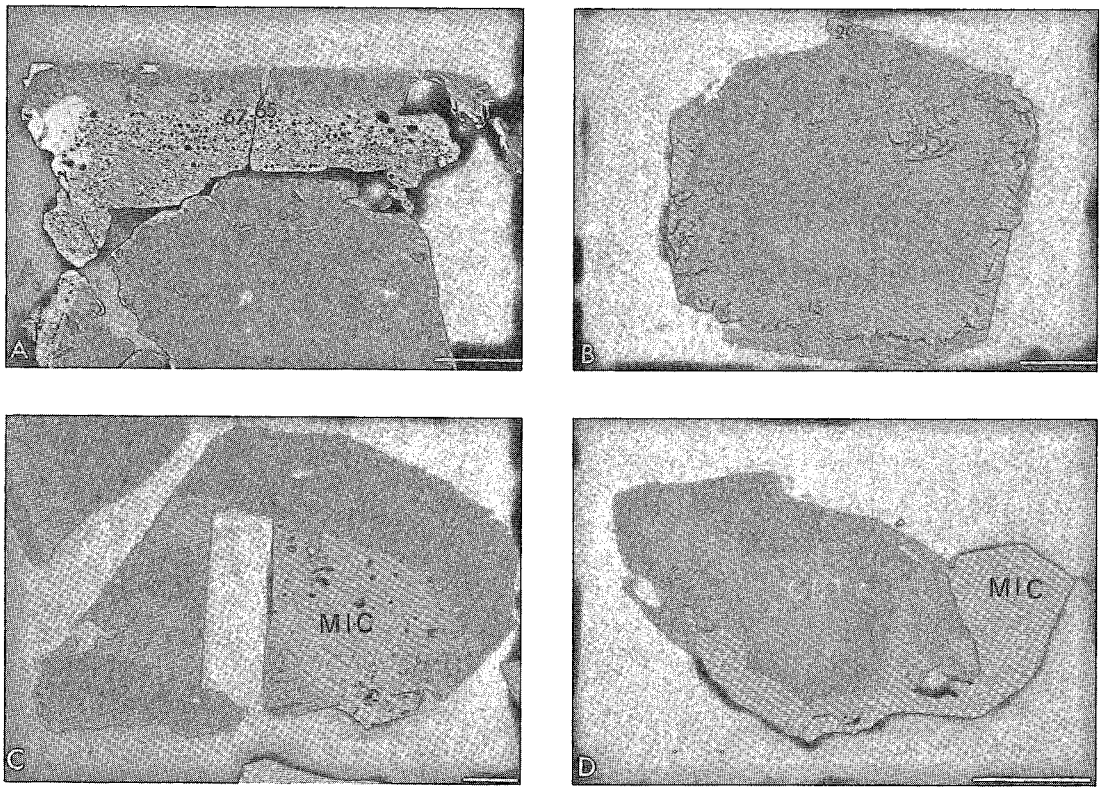

FIG. 2. Aspects of the microlite grains in the Beauvoir granite and their association with columbite-group minerals. Back-scattered electron (BSE) images. Bar scales are expressed in μm. A. Pyrochlore crystal showing a porous margin enriched in Ta, represented by the light band on the photo. The points indicate the locations of the spot-analyses (Table 1). B. Zoned grain, with lobes resulting from hydration. The alternating light and dark bands are growth zones rich in tantalum and in niobium, respectively. C, D. Relations between microlite (MIC) and columbite- and tantalite-group minerals (CBTA). Partly magmatic resorption of microlite enclosed in manganocolumbite, and zoned columbite partly rimmed and replaced by microlite. The microlite in the lower part cuts the growth zoning of the manganocolumbite–ferrocolumbite.

tends to replace the pre-existing manganocolumbite. This phenomenon also was observed in granitic pegmatites from Greer Lake, Manitoba (Černý & Turnock 1971, Černý *et al.* 1986), and from Yellowknife, Northwest Territories (Wise & Černý 1990), and in lepidolite – amazonite – albite granites of Siberia (Sitnin & Bykova 1962), and in rare-metal pegmatites from Namibia and South Africa (Baldwin 1989).

CRYSTAL CHEMISTRY OF THE PYROCHLORE-GROUP MINERALS

Analytical methods

A systematic study of the pyrochlore-group minerals was carried out on thin and polished sections of samples from the drill-hole. Grains were photographed by back-scattered electron image (BSE) on the BRGM Cambridge Stereoscan 250 scanning electron microscope and analyzed on the CNRS–BRGM and CNRS – Université d'Orléans – BRGM Camebax electron microprobes (EPMA). The analytical conditions were as follows: acceleration potential 20 kV, reference current 12 nA, counting time 10 s per element. The following standards were used: microlite (Ingamells 1978) for Na*K*α, F*K*α, Ca*K*α and Ta*M*α, UO_2 for U*M*α, orthoclase for K*K*α, $LiNbO_3$ for Nb*L*α, W metal for W*M*α, synthetic SnO_2 for Sn*L*α, synthetic Fe_2O_3 for Fe*K*α, synthetic $MnTiO_3$ for Mn*K*α and Ti*K*α, and PbS for Pb*M*α. The ZAF correction program used was MBXCOR of Henoc & Tong (1978). Using the method of Ancey *et al.* (1978), the calculated relative confidence-interval at 99% is a few percent for major elements and reaches 30% for trace elements. The structural formula was calculated according to the method recommended by Borodin & Nazarenko (1957),

TABLE 1. REPRESENTATIVE COMPOSITIONS OF PYROCHLORE-GROUP MINERALS FROM THE BEAUVOIR GRANITE

	1	2	3	4	5	6	7	8	9	10	11	12	13	14	15	16
Depth m	132.95	132.95	132.95	132.95	132.95	132.95	260.00	260.00	298.00	298.00	298.00	498.00	498.00	498.00	550.00	567.75
Probe n°	63	65	67	68	71	74	185	186	15	16	20	125	127	128	71	38
Weight percent																
Nb2O5	27.54	23.86	23.39	30.26	32.56	38.01	15.57	9.93	11.34	18.91	19.12	9.01	12.17	16.46	4.26	3.68
Ta2O5	48.97	57.04	56.37	45.50	44.90	36.32	63.15	67.40	64.30	56.66	51.87	63.82	60.14	53.53	68.44	72.89
WO3	2.13	1.62	1.35	2.92	4.63	2.49	2.72	2.76	2.91	2.83	2.01	2.45	1.11	1.14	2.24	1.92
TiO2	0.00	0.00	0.00	0.00	0.00	0.00	0.00	0.07	0.00	0.00	0.05	0.04	0.24	0.52	0.10	0.18
SnO2	0.21	0.29	0.01	0.39	0.22	0.39	0.33	0.31	0.44	0.42	0.65	0.67	0.55	0.92	1.37	0.75
UO2	2.20	2.11	2.02	1.70	1.21	5.68	0.18	1.36	4.63	2.38	10.80	8.82	11.83	12.94	9.92	11.54
FeO	0.00	0.00	0.00	0.00	0.05	0.00	0.00	0.00	0.00	0.00	0.00	0.00	0.00	0.00	0.08	0.00
MnO	0.00	0.05	0.00	0.02	0.02	0.00	0.00	0.07	0.00	0.05	0.13	0.10	0.00	0.00	0.00	0.83
CaO	10.67	0.00	10.37	10.35	10.73	9.46	10.32	9.72	8.24	9.42	3.62	6.51	5.67	5.62	6.06	1.32
PbO	0.00	0.00	0.00	0.00	0.00	0.03	0.00	0.00	0.00	0.00	4.84	0.52	0.58	0.70	0.27	0.19
Na2O	5.44	3.30	3.56	5.77	3.81	4.74	5.97	4.94	3.94	4.86	0.41	3.52	3.39	3.34	2.60	0.08
K2O	0.02	0.14	0.01	0.00	0.00	0.09	0.00	0.00	0.02	0.00	0.29	0.05	0.00	0.00	0.00	0.55
F	3.53	2.71	4.35	4.25	4.00	3.36	2.70	2.95	2.68	3.49	0.50	1.53	0.10	1.36	0.97	0.00
H2O	0.26	0.36	0.00	0.00	0.11	0.42	0.56	0.34	0.43	0.15	1.37	0.90	1.59	1.03	1.11	1.47
O=F	1.49	1.14	1.83	1.79	1.68	1.41	1.14	1.24	1.13	1.47	0.21	0.64	0.04	0.57	0.41	0.00
Total	99.49	90.34	99.60	99.37	100.55	99.57	100.36	98.61	97.80	97.70	95.45	97.30	97.33	96.99	97.01	95.40
Structural formula calculated on the basis of Ta+Nb+Ti+W=2																
Nb	0.95	0.81	0.81	1.02	1.05	1.24	0.56	0.38	0.44	0.69	0.74	0.37	0.49	0.66	0.18	0.15
Ta	1.01	1.16	1.17	0.92	0.87	0.71	1.38	1.55	1.50	1.25	1.21	1.57	1.47	1.28	1.76	1.79
W	0.04	0.03	0.03	0.06	0.09	0.05	0.06	0.06	0.06	0.06	0.04	0.06	0.03	0.03	0.05	0.04
Ti	0.00	0.00	0.00	0.00	0.00	0.00	0.00	0.00	0.00	0.00	0.00	0.00	0.02	0.03	0.01	0.01
Sn	0.01	0.01	0.00	0.01	0.01	0.01	0.01	0.01	0.02	0.01	0.02	0.02	0.02	0.03	0.05	0.03
U	0.04	0.04	0.03	0.03	0.02	0.09	0.00	0.03	0.09	0.04	0.21	0.18	0.24	0.25	0.21	0.23
Fe	0.00	0.00	0.00	0.00	0.00	0.00	0.00	0.00	0.00	0.00	0.00	0.00	0.00	0.00	0.01	0.00
Mn	0.00	0.00	0.00	0.00	0.00	0.00	0.00	0.01	0.00	0.00	0.01	0.01	0.00	0.00	0.00	0.06
Ca	0.87	0.00	0.85	0.83	0.82	0.73	0.89	0.88	0.76	0.82	0.33	0.63	0.54	0.53	0.61	0.13
Pb	0.00	0.00	0.00	0.00	0.00	0.00	0.00	0.00	0.00	0.00	0.11	0.01	0.01	0.02	0.01	0.00
Na	0.80	0.48	0.53	0.83	0.53	0.66	0.93	0.81	0.65	0.76	0.07	0.62	0.59	0.57	0.48	0.01
K	0.00	0.01	0.00	0.00	0.00	0.01	0.00	0.00	0.00	0.00	0.03	0.01	0.00	0.00	0.00	0.06
Total A	1.72	0.54	1.41	1.70	1.37	1.51	1.83	1.74	1.51	1.64	0.78	1.48	1.40	1.40	1.36	0.53
F	0.85	0.64	1.05	1.00	0.90	0.76	0.68	0.79	0.72	0.89	0.13	0.43	0.03	0.37	0.28	0.00
OH	0.15	0.36	0.00	0.00	0.10	0.24	0.32	0.21	0.28	0.11	0.87	0.57	0.97	0.63	0.72	1.00

Columns 1 to 5: zones in the crystal shown in Figure 2A. The margin (1) is richer in tantalum than the core (5). The porous zone (2) and tantalum-rich rim (1) that border the porous zone have a composition close to ideal microlite. Column 6 shows the composition of end-member pyrochlore analyzed. Columns 7 and 8 pertain to the core and margin of a single crystal. Column 11 is the margin, rich in U and enriched in Pb, of a crystal (9, 10) in which leaching is well developed (Fig. 2B). Columns 12 to 14 show the variations from the core to the margin of a single crystal, 15 is a uranmicrolite from the bottom of the drill hole, and 16 is a metamict uranmicrolite.

Van Wambecke (1970) and Lumpkin *et al.* (1986); it assumes that the sum of the cations ($Nb^{5+} + Ta^{5+} + W^{6+} + Ti^{4+}$) occupying *B* sites is equal to 2. F was measured and OH calculated assuming full occupancy of the *Y* site. All the analytical data, from about 300 analyses, are available upon request or through the Depository of Unpublished Data, Canada Institute for Scientific and Technical Information, National Research Council, Ottawa, Canada K1A 0S2. Representative compositions are given in Table 1.

Crystal chemistry

Minerals of the pyrochlore group have as general formula $A_{2-m}B_2X_6Y_{1-n}\bullet pH_2O$ (Hogarth 1977, Lumpkin *et al.* 1986), where *A* may be occupied by Na, Ca, U, Pb, Sr, Th, *REE*, Bi, Sn^{2+}, Ba, Mn, and Fe^{2+}, *B*, by Ta, Nb, Ti, Zr, Fe^{3+}, Sn^{4+} and W; *X* stands for oxygen atoms, and *Y*, for O, OH and F; m has a value from 0 to 2, n, from 0 to 1 and p, from 0 to 1 (?). Structural vacancies may appear in sites *A* and *Y*. Hogarth (1977) defined three subgroups on the basis of Ta, Nb and Ti contents, as follows: the microlite subgroup, with Ta ≥ Nb and Nb + Ta >2Ti, the pyrochlore subgroup, with Nb>Ta and Nb + Ta>2Ti, and the betafite subgroup, with 2Ti ≥ Nb + Ta (Fig. 3A).

The structure of pyrochlore is a derivative of that of fluorite (Pyatenko 1959, Chakoumakos 1984) within the cubic space-group *Fd3m*, with a deficit in anions. It is composed of a framework of BO_6 octahedra linked at their summits and interpenetrated by a network of A_2Y chains (Ercit *et al.* 1985). The seventh oxygen atom and the *A* cations are not essential for the stability of the structure (Gaspérin 1960), thus enabling easy migration of ions in the *A* and *Y* sites (Subramanian *et al.* 1983). An increased content of water (Foord 1982) is generally correlated with a deficit at the *A* site. The transformation of these minerals to a metamict state is widespread (Lumpkin *et al.* 1986). It provokes strong variations in their composition, marked by a loss of ions from the *A* site, and the entry of the large-radius cations K, Sr, Ba and Pb, and H_2O (Van der Veen 1963).

B-site cations

Pentavalent Ta and Nb are the main cations at the *B* sites, with the majority of data points projecting in the microlite field. The amount of Ta, in number of atoms per standard formula unit (a.s.f.u.), ranges between 0.71

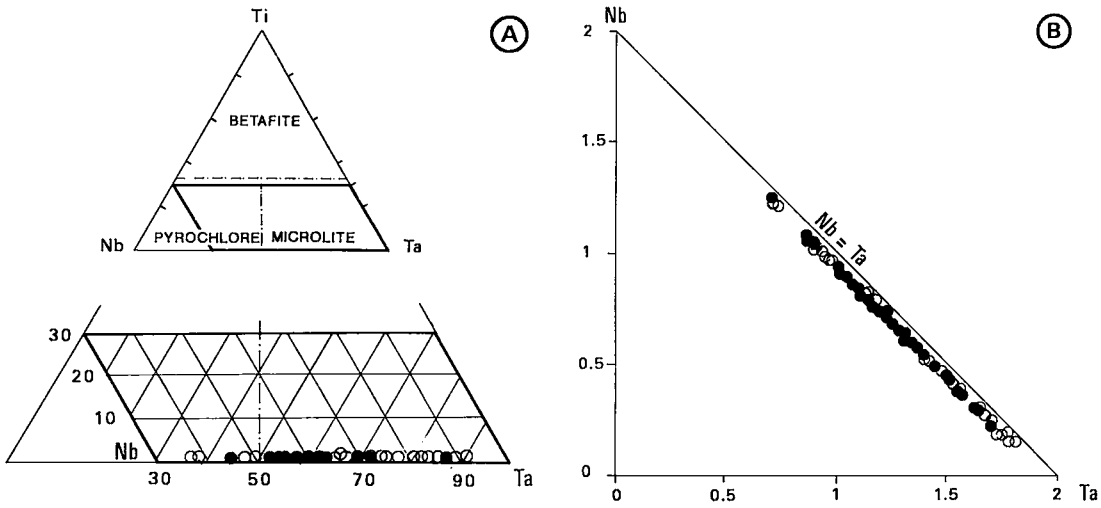

FIG. 3. A. Pyrochlore classification of Hogarth (1977) according to the major elements in site *B*. B. Isovalent Nb^{5+} – Ta^{5+} substitution in site *B*. Dots represent nonmetamict microlite (total >98%), and open circles, metamict and hydrated microlite.

and 1.80, and of Nb, between 0.15 and 1.21. The ratio Ta/Nb in microlite decreases, from bottom to the top of the drill-hole. There is limited replacement of Ta and Nb by Ti, ranging from 0 to 0.03 a.s.f.u., and, to a lesser extent, W (0 – 0.08 a.s.f.u.). The Ta–Nb diagram (Fig. 3B) illustrates that Nb and Ta almost completely fill the B position. The data fall on a line of slope 1, parallel to the ideal Nb–Ta substitution. Nb and Ta occupy 96.5% of the *B* sites, whereas Ti^{4+} and W^{6+} occupy the remaining 3.5%.

A-site cations

The principal cations occupying the *A* site are Ca and Na, which range from 0 to 0.99 and from 0.01 to 0.99 a.s.f.u., respectively. Other cations (U, Sn, Pb, K) do not exceed, on the average, 20% of the population of the *A* site. As shown by Vorna & Siivola (1967) and Ercit *et al.* (1987), Sn in stannomicrolite is predominantly Sn^{2+}. In the Beauvoir leucogranite, SnO_2 content is generally low, with Sn occupying 0 to 0.06 a.s.f.u. For non-hy-

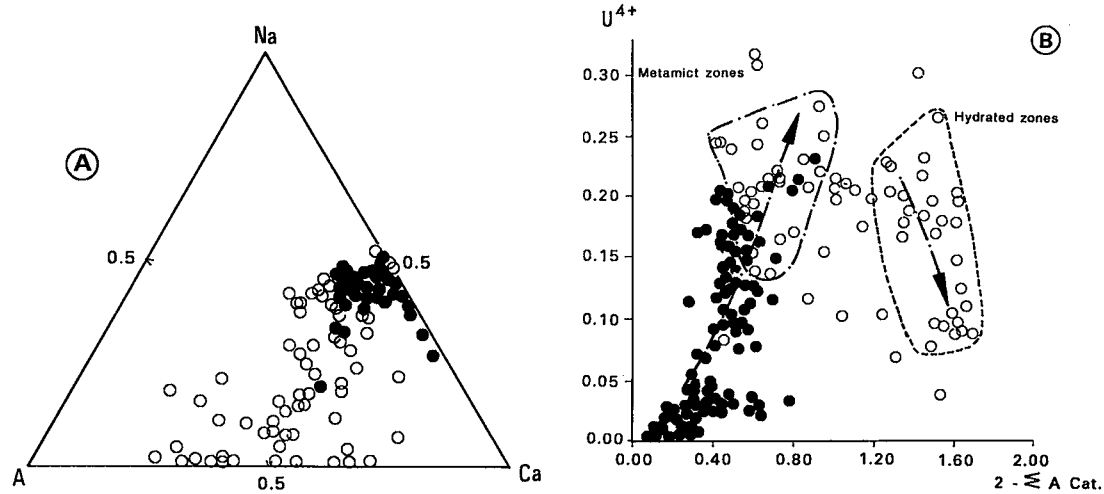

FIG. 4. A. Occupancy of site *A*. Comparison between Na^+ and Ca^{2+} and the sum of the other *A*-site cations. B. Comparison between the deficit in the *A*-site and the amount of U present in the site.

drated samples, the average occupancy of the *A* site is 81%, whereas two maxima are observed for hydrous samples. 1) One of these has an occupancy of 74%, the decrease in the occupancy possibly resulting from metamictization. In pyrochlore-group minerals, the degree of hydration may be correlated with metamict character (Barsanov 1957, Gromet & Silver 1983). 2) The second maximum corresponds to almost complete leaching of the *A* site, resulting in an occupancy of only 28%, and would represent the strongly hydrated botryoidal and colloform zones that commonly form during weathering of pyrochlore ("marignacitization" of Barsanov 1945). The phenomenon of selective leaching, which particularly affects Na and Ca, explains the relatively high occupancy of the *A* site by the remaining ions (Fig. 4A), which may reach 75%, when this site is highly deficient (Borodin & Nazarenko 1957). The increase in the number of vacancies at the *A* site is related to the presence of uranium in this site. The uranium content decreases in microlite from the bottom to the top of the drill-hole. When half of the *A* site is vacant, the uranium has been leached (Fig. 4B). Hogarth (1989) came to the same conclusion for pyrochlore in carbonatites, from which the uranium is removed in the most advanced stages of weathering. Alkali cations are preferentially removed relative to the alkaline earths, as shown in the Na *versus* Ca diagram (Fig. 4A).

Substitution scheme

Apart from the obvious scheme of substitution $Ta^{5+} \leftrightarrow Nb^{5+}$ at the *B* site (Fig. 3B), which is not affected by mineral hydration, this study has revealed another important substitution involving U^{4+} and Ca^{2+} (Fig. 5A). The correlation coefficient *r* obtained for the group of non-hydrated pyrochlore-group minerals is –0.97. The substitution of U^{4+} for Ca^{2+} is accompanied by a loss of Na^+ (Fig. 5B) and F (Figs. 5E, 5F) at the *Y* site.

Lumpkin *et al.* (1986) have proposed substitution schemes for microlite from the Harding pegmatite. In particular, they showed positive correlations between Na and F, and between $\square_A$ and $\square_Y$, and a negative correlation between U and F. Based on the high U^{6+}/U^{4+} ratio in these grains of microlite (Jahns & Ewing 1976), Lumpkin *et al.* (1986) proposed that uranium in microlite is U^{6+} and that it is present at the *A* site in the form of the uranyl group (UO_2^{2+}). In microlite of the Beauvoir granite, the local association of uraninite with microlite suggests that uranium may be present as U^{4+}. A major scheme of substitution involving U^{4+} also has been proposed by Hogarth & Thorne (1989) for the non-metamict uranpyrochlore and uranoan pyrochlore of Ndale, Uganda and by Baldwin (1989) for the uranoan microlite of Kokerboomrand, South Africa. This substitution is of the heterovalent type: $3Nb^{5+} + Na^+ \leftrightarrow 3Ti^{4+} + U^{4+}$ for pyrochlore and $3Ta^{5+} + Na^+ \leftrightarrow 3Ti^{4+} + U^{4+}$ for microlite, similar to the "betafite scheme" ($Ca^{2+} + 2Nb^{5+} \leftrightarrow U^{4+} + 2Ti^{4+}$) and opposite of the "uranpyrochlore scheme": $2Ca^{2+} \leftrightarrow U^{4+} + \square$ (Hogarth 1989). The presence in the Beauvoir granite of tetravalent uranium in the major heterovalent substitutions is confirmed in the *A* site by the U–Ca diagram, in which the points are aligned along a line of slope –3/4. To account for the fact that Ca and Na increase simultaneously (Figs. 5A, B, C), a scheme of substitution of the type $3U^{4+} + 5\square_A \leftrightarrow 4Na^+ + 4Ca^{2+}$, or, more generally, $3U^{4+} + 5\square_A \leftrightarrow 8(Na^+, Ca^{2+})$ is proposed for the *A* site. In keeping with the loss of F^- recorded with the increase in U^{4+}, this substitution is probably accompanied by a rearrangement at the *Y* site, with the creation of vacancies and substitution of O^{2-} for $2F^-$ or of OH^- for F^-. Also, the U–Sn, U–F and Sn–F correlations (Figs. 5D, E, F) indicate that the behavior of tin is similar to that of uranium; it could be replaced by calcium at the *A* site. The extent of substitution $2(Nb,Ta)^{5+} \leftrightarrow Ti^{4+} + W^{6+}$ in site *B* must be limited. The content of W^{6+} is always greater than that of Ti^{4+}, and thus tungsten should replace the pentavalent cations in the *B* site according to the coupled substitution:

$$^{B}W^{6+} + {}^{Y}O^{2-} \leftrightarrow {}^{B}(Nb,Ta)^{5+} + {}^{Y}F^-.$$

The substitutions in the Beauvoir microlite may thus be written:

$$^{A}[(Na^+, Ca^{2+})_{2-8/3x}U^{4+}_x\square_{5/3x}]$$
$$^{B}[(Ta^{5+}, Nb^{5+})_{2-y}W^{6+}]\ X_6\ ^{Y}[(F^-_{1+y-z}OH^-_z), O^{2-}_{1-y}]$$

with $x \leq 3/4$.

The incorporation of U at the *A* site implies the existence of an $U^{4+}Ta^{5+}{}_2O^{2-}{}_7$ end member, previously proposed by Gaspérin (1960) and Lumpkin *et al.* (1986).

Zoning, metamictization and replacement of microlite

The microlite crystals show two main types of chemical variation that are visible either as zoning or as spots due to hydration and leaching along fractures (Figs. 6A, B, C, D). Oscillatory growth-zoning takes the form of uniform bands from a few to several tens of micrometers in width (Fig. 6B). The compositional variations are governed by the substitutions discussed above. Two microprobe traverses were made across a strongly oscillatory-zoned crystal (Figs. 6B, C, 7A, B); representative compositions are given in Table 2. The oscillatory growth-zoning is marked by Nb-for-Ta substitution (Fig. 7C). W behaves sympathetically with Ta; Na, Ca and F have the same pattern of distribution, with complete leaching of these elements in the metamict zones (Fig. 7C). The core of the crystal is enriched in U and Sn.

FIG. 5. Variation diagrams showing the atoms per standard formula unit (a.s.f.u.) for $A_{2-m}B_2X_6Y_{1-n}\bullet pH_2O$. A) U^{4+} *versus* Ca^{2+}, B) Ca^{2+} *versus* Na^+, C) U^{4+} *versus* $Ca^{2+} + Na^+$, D) U^{4+} *versus* Sn^{2+}, E) U^{4+} *versus* F^-, F) Sn^{2+} *versus* F^-.

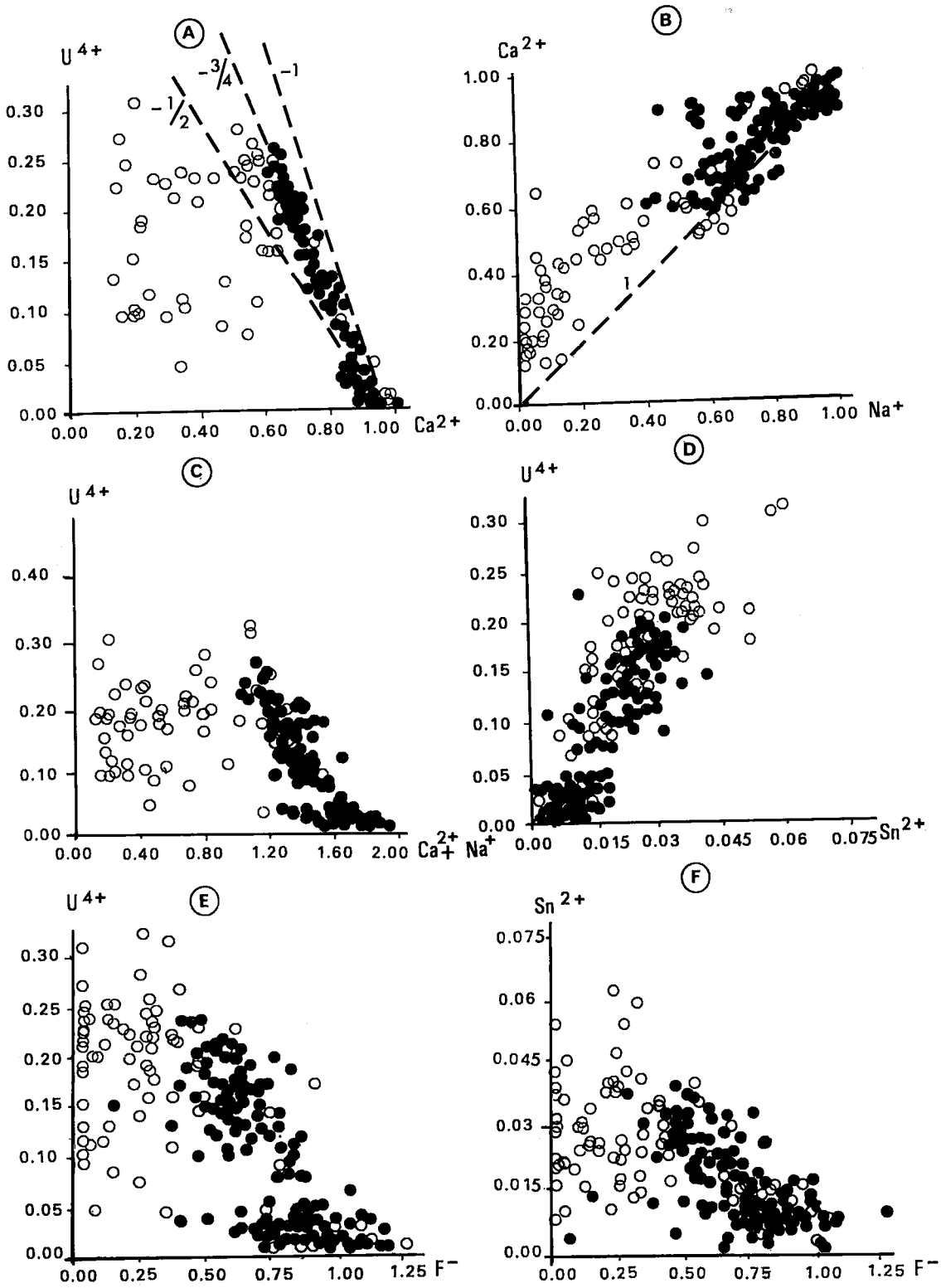
A
U 4+
-1/2
-3/4
-1
0.30
0.25
0.20
0.15
0.10
0.05
0.00
0.00 0.20 0.40 0.60 0.80 1.00 Ca2+
B
Ca 2+
1.00
0.80
0.60
0.40
0.20
0.00
1
0.00 0.20 0.40 0.60 0.80 1.00 Na+
C
U 4+
0.40
0.30
0.20
0.10
0.00
0.00 0.40 0.80 1.20 1.60 2.00 Ca2+ Na+
D
U 4+
0.30
0.25
0.20
0.15
0.10
0.05
0.00
0.00 0.015 0.03 0.045 0.06 0.075 Sn2+
E
U 4+
0.30
0.25
0.20
0.15
0.10
0.05
0.00
0.00 0.25 0.50 0.75 1.00 1.25 F−
F
Sn 2+
0.075
0.06
0.045
0.03
0.015
0.00
0.00 0.25 0.50 0.75 1.00 1.25 F−

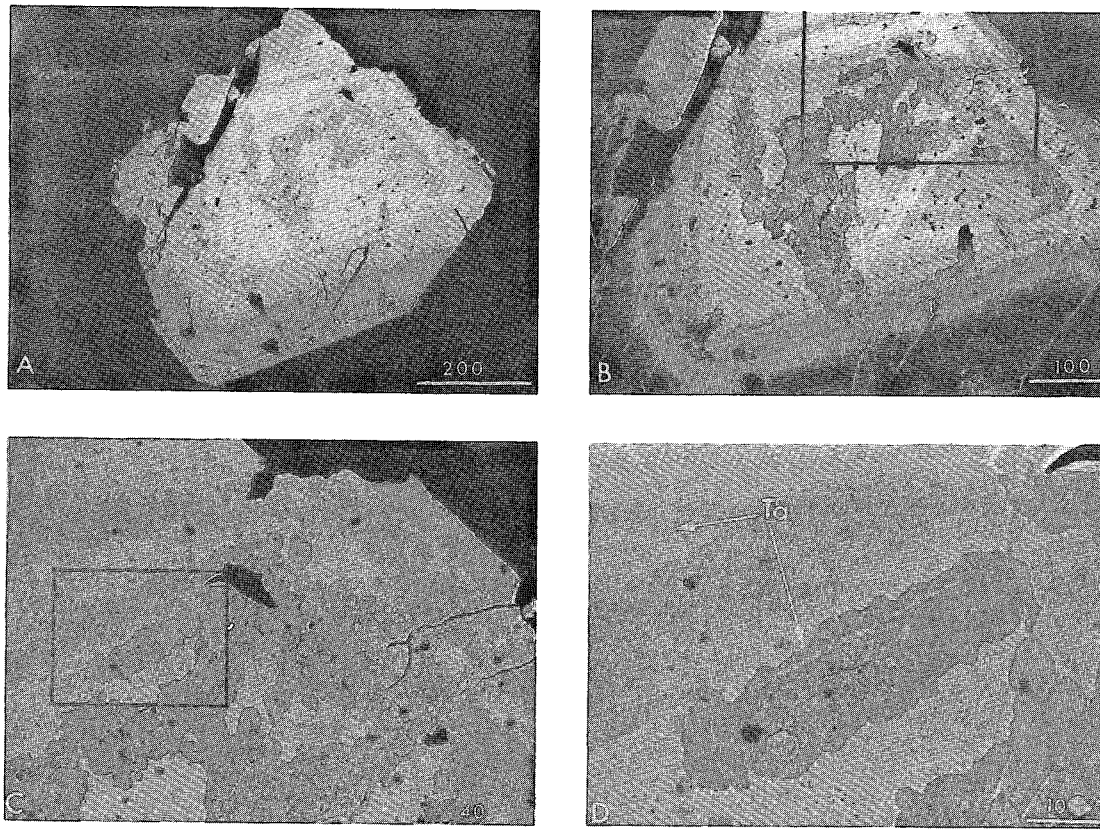

FIG. 6. BSE images of a microlite crystal sampled at 110 m. Bar scales are expressed in μm. Oscillatory growth zones are marked by lighter parallel bands; the dark core is richer in U. Metamictization and hydration take place preferentially in this zone. The processes start from irregular microveinlets and develop along darker lobes that cut across the primary structure of the crystal. The detailed view of the metamict and hydrated zone (Figs. 6C, D) shows preserved polygonal granular aggregates of microlite isolated by leaching that occurs during the hydration of the crystal. The white rims to the lobes of alteration are due to enrichment in Ta. Fine late veinlets (anal. 17, Table 2) enriched in Ta (white) cut all other structures.

In addition to this zoning due to primary petrogenetic processes, the phenomenon of metamictization also has exerted a major influence on composition. Metamictization results from radiation damage caused by alpha particles generated by uranium atoms (Ewing 1975) within the microlite structure. Where microlite contains less than 2 wt% of UO_2, no sign of metamictization is observed. On the other hand, where UO_2 is abundant (Figs. 5, 7), granular zones exist, that in plane-polarized light range from dark green to brown. These are the metamict and hydrated parts of the crystal, respectively. These zones appear darker grey than the unaltered mineral in polished section. The BSE image clearly shows these zones, which appear darker owing to impoverishment in U atoms as well as to a higher proportion of intracrystalline voids associated with structural damage (Krivokoneva & Sidorenko 1971), due to metamictization and the higher proportion of *A*-site vacancies in U-rich samples. The images demonstrate the colloform nature of the products of metamictization and hydration (Figs. 6B, C, D). At the boundaries between the metamict-hydrated and unaltered zones are bands enriched in tantalum comparable to the cross-cutting Ta-enriched veinlets (anal. 17, Table 2). These seems to result from the migration of Ta upon metamictization. In some cases (Figs. 6D, 7B), the advance of metamictization isolates polygonal granular aggregates with compositions very close to those of the

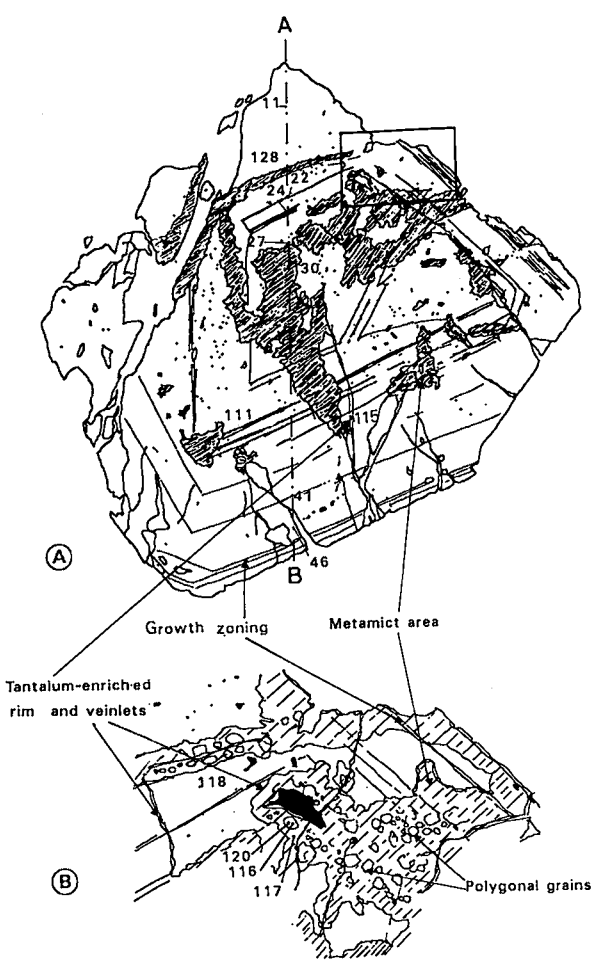

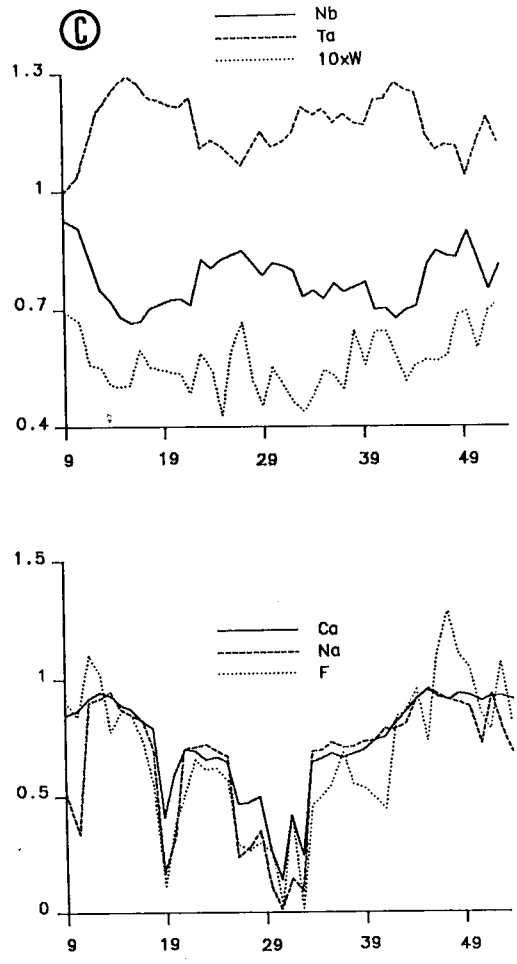

FIG. 7. Diagrams and EPMA profiles for a typical grain of microlite from depth 110 m in facies B_1 of the Beauvoir granite. A. Drawing made from BSE image shows the location of one of the two traverses A–B and the other analyses performed on the crystal (Table 2). The enlargement of the boxed area (B) shows in detail the shape of the grains and Ta-enriched veinlets (anal. 17, Table 2). C. Traverse A–B (Fig. 7A) across the grain. The growth zones are marked mainly by the substitution of Ta^{5+} for Nb^{5+}, W^{6+} tending to follow Ta^{5+}. The close agreement between Na^{+}, Ca^{2+} and F^{-} profiles is related on the one hand to the incorporation of U^{4+} into the *A* sites and, on the other hand, by the leaching of the same *A* site, which may be practically complete. U and Sn are concentrated in the center of the crystal and show parallel trends of enrichment. The Sn values have been multiplied by 6. The numbers given on the abscissa are those of the analyses reported in Table 2. On the ordinate, proportions of the cations are normalized to a total occupancy of *B* site equal to 2.

TABLE 2. REPRESENTATIVE COMPOSITIONS OF THE ZONED CRYSTAL OF MICROLITE FROM 110.30 m

	1	2	3	4	5	6	7	8	9	10	11	12	13	14	15	16	17
Probe n°	11	22	24	27	30	36	45	46	99	111	116	117	118	120	128	130	115
Weight percent																	
Nb2O5	23.01	21.94	21.54	21.63	22.11	20.41	23.09	23.95	22.74	18.47	20.93	21.39	21.91	19.28	17.72	21.72	19.76
Ta2O5	51.58	49.73	47.97	44.80	49.67	51.49	53.43	51.50	52.97	54.08	49.81	51.63	50.28	52.72	56.07	46.14	60.05
WO3	2.72	2.75	1.97	2.98	2.63	2.49	2.84	2.81	3.38	1.97	2.77	2.43	2.85	2.37	2.71	2.64	3.03
TiO2	0.00	0.00	0.00	0.00	0.00	0.00	0.00	0.00	0.04	0.00	0.05	0.17	0.00	0.00	0.00	0.00	0.03
SnO2	0.26	0.77	1.13	1.13	1.11	0.82	0.23	0.31	0.31	0.77	0.84	0.53	0.85	0.66	0.71	1.10	0.42
UO2	1.09	8.87	10.64	11.75	11.18	8.72	0.00	0.10	1.15	10.38	10.59	10.06	9.92	8.64	6.16	13.60	4.00
FeO	0.00	0.00	0.00	0.00	0.00	0.00	0.00	0.00	0.04	0.08	1.01	1.03	0.00	0.00	0.00	0.00	0.02
MnO	0.00	0.00	0.00	0.16	0.08	0.00	0.00	0.00	0.00	0.00	0.01	0.26	0.03	0.23	0.00	0.03	0.00
CaO	10.49	7.21	6.97	4.96	1.53	7.30	10.79	10.62	10.46	7.39	6.75	3.87	7.51	6.49	8.91	5.14	4.69
PbO	0.00	0.14	0.35	0.38	0.00	0.20	0.00	0.00	0.00	0.05	0.50	0.48	0.07	1.20	0.18	0.06	0.38
Na2O	5.72	4.38	3.89	1.61	0.08	4.31	6.05	5.85	5.21	4.49	0.26	0.43	4.02	2.31	5.10	1.76	0.28
K2O	0.00	0.02	0.02	0.79	0.54	0.01	0.00	0.00	0.00	0.00	0.18	0.50	0.00	0.38	0.01	0.52	0.27
F	4.30	2.28	2.08	0.93	0.10	2.56	4.42	5.11	3.90	2.12	1.30	0.00	1.61	1.06	2.73	0.87	0.49
H2O	0.00	0.89	0.76	1.19	1.54	0.55	0.00	0.00	0.03	0.76	1.08	1.67	1.04	1.20	0.51	1.26	1.46
O=F	1.81	0.96	0.88	0.39	0.04	1.08	1.86	2.15	1.64	0.89	0.55	0.00	0.68	0.45	1.15	0.37	0.21
Total	97.38	96.82	96.54	91.92	90.53	97.78	98.99	98.10	98.59	99.67	95.33	94.45	99.21	96.09	99.66	94.47	94.67
Structural formula calculated on the basis of Ta + Nb + Ti + W = 2																	
Nb	0.83	0.83	0.84	0.86	0.83	0.77	0.81	0.85	0.80	0.71	0.80	0.79	0.81	0.74	0.67	0.85	0.63
Ta	1.12	1.11	1.12	1.07	1.12	1.17	1.13	1.10	1.13	1.25	1.14	1.15	1.12	1.21	1.27	1.09	1.15
W	0.06	0.06	0.04	0.07	0.06	0.05	0.06	0.06	0.07	0.04	0.06	0.05	0.06	0.05	0.06	0.06	0.06
Ti	0.00	0.00	0.00	0.00	0.00	0.00	0.00	0.00	0.00	0.00	0.00	0.01	0.00	0.00	0.00	0.00	0.16
Sn	0.01	0.03	0.04	0.04	0.04	0.03	0.01	0.01	0.01	0.03	0.02	0.02	0.02	0.02	0.02	0.04	0.01
U	0.02	0.17	0.20	0.23	0.21	0.16	0.00	0.00	0.02	0.20	0.20	0.18	0.18	0.16	0.11	0.26	0.06
Fe	0.00	0.00	0.00	0.00	0.00	0.00	0.00	0.00	0.00	0.01	0.07	0.07	0.00	0.00	0.00	0.00	0.00
Mn	0.00	0.00	0.00	0.01	0.01	0.00	0.00	0.00	0.00	0.00	0.00	0.02	0.00	0.02	0.00	0.00	0.00
Ca	0.89	0.65	0.64	0.47	0.14	0.66	0.90	0.89	0.88	0.67	0.61	0.34	0.66	0.59	0.80	0.48	0.36
Pb	0.00	0.00	0.01	0.01	0.00	0.00	0.00	0.00	0.00	0.00	0.01	0.01	0.00	0.03	0.00	0.00	0.01
Na	0.88	0.71	0.66	0.27	0.01	0.70	0.91	0.89	0.79	0.74	0.04	0.07	0.64	0.38	0.83	0.30	0.04
K	0.00	0.00	0.00	0.09	0.06	0.00	0.00	0.00	0.00	0.00	0.02	0.05	0.00	0.04	0.00	0.06	0.02
Total A	1.80	1.55	1.56	1.12	0.45	1.55	1.82	1.79	1.70	1.64	0.97	0.76	1.51	1.24	1.77	1.14	0.50
F	1.08	0.60	0.55	0.25	0.03	0.67	1.08	1.26	0.96	0.56	0.34	0.00	0.41	0.28	0.71	0.23	0.11
OH	0.00	0.40	0.45	0.75	0.97	0.33	0.00	0.00	0.04	0.44	0.66	1.00	0.59	0.72	0.29	0.77	0.89

Columns 1–9 pertain to compositions determined along profile A–B shown in Figure 7A; the other compositions pertain to points shown in Figures 7A and 7B.

non-metamict zone. The process of formation could be comparable to the polygonization observed by Barsanov (1945) in chemically leached pyrochlore, and to the subspheroidal areas in uranoan microlite from the Tantalite Valley, Namibia (Baldwin 1989). The persistence, on the scale of few nanometers, of relict islands of crystalline material in an aperiodic matrix has been observed by HRTEM in metamict microlite of the Harding pegmatite (Lumpkin & Ewing 1988).

This late phenomenon is accompanied by hydration and selective leaching of ions from the *A* sites, with the removal, in order of importance, of Na, Ca, U, and F from the *Y* site. These losses are accompanied by the introduction of large-radius ions such as K^+, Pb^{2+} and Ba^{2+} into the altered microlite (Gaspérin 1972, Kosakevitch 1976). The products of the alteration of microlite may be found in microfractures within the mineral or as a rim around the grains, as observed in exploratory drill-holes (Kosakevitch 1976). This included the formation of apatite through combination of liberated calcium with phosphorus from late-magmatic fluids. A similar complex reaction-rim with apatite, quartz and mica also has been observed around certain grains of microlite from the Beauvoir drill-hole.

Distribution of U in microlite: evidence for two stages of growth

Uranium seems to be the element that best reveals the evolution of the microlite, as represented by compositional zoning. A detailed investigation of the distribution of U in the grains shows two main levels of concentration. In U-poor crystals, the variations are of the order of a few percent (about 2 wt% UO_2), with a slight increase at the border of the crystals (Table 3, Fig. 8). In the U-rich microlite (up to 13.8 wt% of UO_2), U is enriched in the cores. The outer parts of the crystals have about the same values as those of U-poor grains. This type of distribution suggests that at least two generations of microlite are present in the Beauvoir granite: 1) the first period of microlite crystallization is marked by U-rich nuclei in some crystals; 2) the second generation of microlite overgrew the older crystals and appeared as separate nuclei (Fig. 8, Table 3). These two periods of growth could explain the "gap" at about 0.07 a.s.f.u. in the distribution of U (Figs. 5C, D, E).

Discussion and Conclusions

The Beauvoir peraluminous granite is highly specialized, with subeconomic concentrations of disseminated rare metals such as Li, Sn, Ta, Nb and W. The three granitic facies encountered show enrichment in alkalis and halogens from the bottom to the top of the drill-hole (Rossi *et al.* 1987, Cuney *et al.*, unpubl. manuscript). The pyrochlore-group minerals are very sensitive to the physicochemical conditions of their environment of crystallization in the leucogranitic magma.

TABLE 3. REPRESENTATIVE COMPOSITIONS OF A ZONED CRYSTAL OF U-POOR MICROLITE FROM 102 m

	1	2	3	4	5	6	7	8	9
probe n°	147	148	149	150	151	152	154	155	156
Weight percent									
Nb2O5	21.73	22.36	23.67	24.64	21.18	23.35	17.51	21.26	26.41
Ta2O5	56.55	53.58	54.95	53.53	56.07	53.12	59.91	54.05	52.11
WO3	3.28	4.42	3.46	2.90	3.27	1.37	2.40	2.71	3.22
TiO2	0.01	0.00	0.00	0.06	0.00	0.00	0.00	0.00	0.08
SnO2	0.23	0.03	0.36	0.45	0.27	0.08	0.25	0.34	0.44
UO2	1.29	1.67	1.43	2.00	1.46	1.40	1.70	2.16	1.63
FeO	0.00	0.04	0.00	0.00	0.07	0.00	0.08	0.00	0.00
MnO	0.00	0.09	0.00	0.00	0.00	0.00	0.02	0.00	0.02
CaO	9.66	9.89	10.02	10.12	10.30	10.01	10.01	9.75	9.90
PbO	0.00	0.05	0.00	0.00	0.00	0.00	0.00	0.00	0.00
Na2O	4.99	5.27	5.50	5.29	5.01	5.49	4.20	5.33	4.84
K2O	0.00	0.00	0.01	0.00	0.14	0.01	0.07	0.10	0.06
F	3.67	2.71	3.00	1.51	2.41	4.20	4.21	2.34	3.73
H2O	0.14	0.00	0.51	1.22	0.74	0.00	0.00	0.73	0.18
O=F	1.55	1.14	1.26	0.64	1.01	1.77	1.77	0.99	1.57
Total	100.00	98.97	101.65	101.08	99.91	97.26	98.59	97.78	101.05
Structural formula calculated on the basis of Ta+Nb+Ti+W=2									
Nb	0.75	0.78	0.81	0.84	0.75	0.83	0.64	0.77	0.89
Ta	1.18	1.13	1.13	1.10	1.19	1.14	1.31	1.17	1.05
W	0.06	0.09	0.07	0.06	0.06	0.03	0.05	0.05	0.06
Ti	0.00	0.00	0.00	0.00	0.00	0.00	0.00	0.00	0.00
Sn	0.00	0.00	0.01	0.01	0.01	0.00	0.00	0.01	0.01
U	0.02	0.03	0.02	0.03	0.02	0.02	0.03	0.04	0.02
Fe	0.00	0.00	0.00	0.00	0.00	0.00	0.00	0.00	0.00
Mn	0.00	0.01	0.00	0.00	0.00	0.00	0.00	0.00	0.00
Ca	0.80	0.82	0.81	0.82	0.86	0.85	0.86	0.84	0.79
Pb	0.00	0.00	0.00	0.00	0.00	0.00	0.00	0.00	0.00
Na	0.74	0.79	0.80	0.77	0.76	0.84	0.66	0.83	0.70
K	0.00	0.00	0.00	0.00	0.01	0.00	0.00	0.01	0.00
Total A	1.57	1.64	1.64	1.64	1.67	1.71	1.56	1.72	1.53
F	0.89	0.66	0.71	0.36	0.59	1.04	1.08	0.59	0.87
OH	0.11	0.34	0.29	0.64	0.41	0.00	0.00	0.41	0.13

The analytical results were obtained at locations indicated in Figure 8.

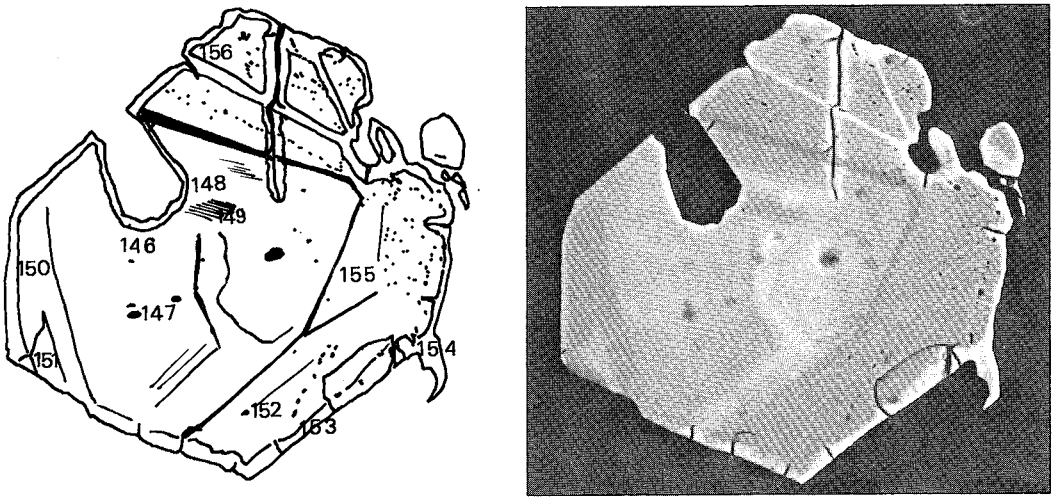

FIG. 8. BSE image of the second generation of a microlite crystal sampled at 102 m. The numbers correspond to those of the analyses in Table 3. Note the Ta enrichment at the rim of the crystal. Scale bar: 20 μm.

Fluorine lowers the solidus temperature of granitic magmas (Wyllie & Tuttle 1961, Manning 1981, London 1987, Webster *et al.* 1987); Li also depresses the solidus (Wyllie & Tuttle 1964, London 1986, 1987). In the case of the Beauvoir leucogranite, the water-saturated solidus temperature at 100 MPa is very low: 575°C and 585°C for facies B1 and B2, respectively (Pichavant *et al.* 1987). Topaz is the first phase on the liquidus, as in the melting experiments on the St. Austell leucogranite (Weidner & Martin 1987). Manning (1981) showed also that increasing concentrations of F in the melt extends the stability field of quartz relative to feldspar. The temperature, deduced from the quartz–lepidolite fractionation in ^{18}O, is estimated to be 570° ± 50°C, very close to the solidus temperature, suggesting early interaction of meteoric fluids with the granitic melt (Fouillac & Rossi 1991). The earliest trapped fluids are brines with 25–30 wt% eq. NaCl, probably enriched in F and Li, with liquid homogenization temperature ranging from 490° to 590°C. These fluids are also very close to the solidus temperature, and indicate that the late-magmatic fluids may be in equilibrium with the crystallizing magma. The depth of emplacement of the Beauvoir leucogranite is estimated of about 3 km (Aïssa *et al.* 1987, Cuney *et al.*, unpubl. manuscript), with a continuous transition from magmatic to hydrothermal systems (London 1986). The high content of fluorine also reduces the viscosity of the magma, and in leucogranitic melts, the distinction between this low-viscosity, fluorine-rich, water-saturated magma and a coexisting fluid phase is diminished (Dingwell *et al.* 1985).

The physicochemical variations due to halogen and alkali enrichment at the end of magmatic differentiation, coupled with the high-temperature, highly saline circulating fluids and the high-temperature interaction of extraneous fluids with the granitic melt, may explain the nonequilibrium crystallization of microlite. Microlite occurs rarely in the lower granitic facies and commonly is included in manganocolumbite – manganotantalite, associated with uraninite as the main carrier of uranium. The decrease in U content from 20 to 12 ppm from bottom to top of the drill-hole could be explained by increasing $f(O_2)$ (Cuney & Brouand 1987). Uraninite disappears between facies B2 and B1, and U is incorporated in the uranoan microlite of the first stage of crystallization. As in the case of the Qaqarsuk carbonatite, Greenland (Knudsen 1989), the evolution from a uranium-rich toward a non-uraniferous microlite could be interpreted as the expression of an increase in the complexing of uranium at the magmatic stage, during the differentiation of the intrusion. Thus the distribution of uranium should reflect an increase in the activity of fluorine, or a variation in $f(O_2)$, or both. In facies B1, where alkalis and halogens are highly concentrated, the replacement of pre-existing manganocolumbite and ferrocolumbite by microlite could be interpreted as a result of metasomatic activity, due to reaction of late magmatic fluids with early Na–Ta oxides (Wise & Černý 1990) according to the reaction AB_2O_6 + Na(F,OH) ↔ pyrochlore in F-rich or alkaline environment (Burt & London 1982). Under these conditions, the second stage of growth of microlite could occur. Oscillatory growth-zoning, common in most of the Beauvoir microlite, reflects diffusion and interface kinematics, with chemical change mainly in Nb and Ta in the granitic magma. The nonequilibrium crystallization of microlite in facies B1 could be related to iron enrichment in columbite by step zoning (Ohnenstetter & Piantone 1988) and in micas (Monier *et al.* 1987); it probably indicates an abrupt change in the physicochemical conditions during crystallization of the leucogranite, due to interaction with meteoric fluid. Very late circulating fluids trapped in inclusions having a low temperature of homogenization and low to moderate salinities (Aïssa *et al.* 1987) could be responsible for late migration of Ta in microlite. The solubilities of Nb and Ta depend on the pH of the medium, Ta being more soluble under acid conditions (Aleksandrov *et al.* 1985).

Acknowledgements

This work was carried out in the framework of the "Géologie Profonde de la France" program, Echassières n° 1 (Thème 8, Evolution of a granitic cupola). We thank all those whose participation enabled this work to be completed. In particular, we are grateful to A. Kosakevitch, who initiated the study and who took part in the acquisition of some of the analytical data, to C. Gilles, who performed some of the microprobe analyses, and J. Breton, who provided the SEM images, to A. Autran, F. Cesbron, P. Černý, C. Fontaine, Z. Johan, M. Pichavant, L. Richard and D.H. Watkinson for critical reviews of the paper, and to J. Kemp and S. Altmann for translation. The two anonymous referees, as well as the editor, R.F. Martin, are thanked for their careful review and improvement of an earlier draft of the manuscript.

References

Aïssa, M., Marignac, C. & Weisbrod, A. (1987): Caractéristiques chimiques et thermodynamiques des circulations hydrothermales du site d'Echassières. *Géol. France* **2-3**, 335-350.

Aleksandrov, I.V., Krasov, A.M. & Kochnova, L.N. (1985): The effects of potassium, sodium and fluorine on rock-forming mineral assemblages and the formation of tantal-niobate mineralization in rare-metal granite pegmatites. *Geochem. Int.* **22**(8), 85-94.

Ancey, M., Bastenaire, F. & Tixier, R. (1978): Application des méthodes statistiques en microanalyse. *In* Microanalyse et microscopie électronique à balayage (F. Maurice, L. Meny et R. Tixier, eds.). Les éditions de physique, Orsay (323-347).

AUBERT, G. (1969): Les coupoles granitiques de Montebras et d'Echassières (Massif Central français) et la genèse de leurs minéralisations en étain, tungstène, lithium et beryllium. *Bur. Rech. Géol. Min., Mém.* **46**.

BALDWIN, J.R. (1989): Replacement phenomena in tantalum minerals from rare-metal pegmatites in South Africa and Namibia. *Mineral. Mag.* **53**, 571-581.

BARSANOV, G.P. (1945): On the secondary alteration of pyrochlore. *Dokl. Akad. Nauk SSSR* **49**, 136-139 (in Russ.).

_____ (1957): Structural features of the structure of metamict niobotantalites. *Trudy Mineral. Muz. Akad. Nauk SSSR* **8**, 3-16 (in Russ.).

BORODIN, L.S. & NAZARENKO, I.I. (1957): Chemical composition of pyrochlore and diadochic substitution in the $A_2B_2X_7$ molecule. *Geochem.* **4**, 330-349.

BURT, D.M. & LONDON, D. (1982): Subsolidus equilibria. *In* Granitic Pegmatites in Science and Industry (P. Černý, ed.). *Mineral. Assoc. Can., Short-Course Handbook* **8**, 329-346.

ČERNÝ, P. & ERCIT, T.S. (1985): Some recent advances in the mineralogy and geochemistry of Nb and Ta in rare-element granitic pegmatites. *Bull. Minéral.* **108**, 499-532.

_____ & _____ (1989): Mineralogy of niobium and tantalum: crystal chemical relationships, paragenetic aspects and their economic implications. *In* Lanthanides, Tantalum and Niobium (P. Möller, P. Černý & F. Saupé, eds.). Springer Verlag, Berlin (27-79).

_____, GOAD, B.E., HAWTHORNE, F.C. & CHAPMAN, R. (1986): Fractionation trends of the Nb- and Ta-bearing oxide minerals in the Greer Lake pegmatitic granite and its pegmatite aureole, southeastern Manitoba. *Am. Mineral.* **71**, 501-517.

_____ & TURNOCK, A.C. (1971): Nobium–tantalum minerals from granitic pegmatites at Greer Lake, southern Manitoba. *Can. Mineral.* **10**, 755-772.

CHAKOUMAKOS, B.C. (1984): Systematics of the pyrochlore structure type, ideal $A_2B_2X_6Y$. *J. Solid State Chem.* **53**, 120-129.

CUNEY, M., AUTRAN, A., BURNOL, L., BROUAND, M., DUDOIGNON, P., FEYBESSE, J.L., GAGNY, C., JACQUOT, T., KOSAKEVITCH, A., MARTIN, P., MEUNIER, A., MONIER, G. & TEGYEY, M. (1986): Résultats préliminaires apportés par le sondage GPF sur la coupole de granite albitique à topaze–lépidolite de Beauvoir (Massif Central, France). *C.R. Acad. Sci. Paris* **303** (sér. II), 569-574.

_____ & BROUAND, M. (1987): Minéralogie, et géochimie de U–Th dans le granite de Beauvoir et les micaschistes encaissants. Comparaison avec la géochimie de l'étain. *Géol. France* **2-3**, 247-254.

DINGWELL, D.B., SCARFE, C.M. & CRONIN, D.J. (1985): The effect of fluorine on viscosities in the system Na_2O–Al_2O_3–SiO_2: implications for phonolites, trachytes and rhyolites. *Am. Mineral.* **70**, 80-87.

DUTHOU, J.L. & PIN, C. (1987): Étude isotopique Rb/Sr de l'apex granitique d'Échassières (granite des Colettes, granite de Beauvoir). *Géol. France* **2-3**, 63-67.

ERCIT, T.S., ČERNÝ, P. & HAWTHORNE, F.C. (1985): Normal and inverse pyrochlore group minerals. *Geol. Assoc. Can. – Mineral. Assoc. Can., Program Abstr.* **10**, A17.

_____, _____ & SIIVOLA, J. (1987): The composition of stannomicrolite. *Neues Jahrb. Mineral. Monatsh.*, 249-252.

EWING, R.C. (1975): The crystal chemistry of complex niobium and tantalum oxides. IV. The metamict state: discussion. *Am. Mineral.* **60**, 728-733.

FEYBESSE, J.J. & TEGYEY, M. (1987): Evolution tectométamorphique dévonienne et carbonifère de la série de la Sioule. *Géol. France* **2-3**, 33-41.

FOORD, E.E. (1982): Minerals of tin, titanium, niobium and tantalum in granitic pegmatites. *In* Granitic Pegmatites in Science and Industry (P. Černý, ed.). *Mineral. Assoc. Can., Short-Course Handbook* **8**, 187-238.

FOUILLAC, A.M. & ROSSI, P. (1991): Near solidus $\delta^{18}O$ depletion in a Ta–Nb bearing albite granite: the Beauvoir granite, France. *Econ. Geol.* **86**, 1704-1720.

GASPÉRIN, M. (1960): Contribution à l'étude de quelques oxydes doubles que forme le tantale avec l'étain, l'uranium et le calcium. *Bull. Soc. Fr. Minéral. Cristallogr.* **83**, 1-21.

_____ (1972): Contribution à l'étude de l'état métamicte: la "néotantalite", une espèce discréditée. *Bull. Soc. Fr. Minéral. Cristallogr.* **95**, 451-457.

GROMET, P.L. & SILVER, L.T. (1983): Rare earth element distributions among minerals in a granodiorite and their petrogenetic implications. *Geochim. Cosmochim. Acta* **47**, 925-939.

HENOC, J. & TONG, M. (1978): Automatisation de la microsonde. *J. Microsc. Electron.* **3**, 247-254.

HOGARTH, D.D. (1977): Classification and nomenclature of the pyrochlore group. *Am. Mineral.* **62**, 403-410.

_____(1989): Pyrochlore, apatite and amphibole: distinctive minerals in carbonatite. *In* Carbonatites: Genesis and Evolution (K. Bell, ed.). Unwin Hyman, London (105-148).

_____ & THORNE, J.E.T. (1989): Non-metamict uranoan pyrochlore and uranpyrochlore from tuff near Ndale, Fort Portal area, Uganda. *Mineral. Mag.* **53**, 257-262.

INGAMELLS, C.O. (1978): Analyzed minerals for electron microprobe standards. *Geostandards Newslett.* **11**, 115.

JAHNS, R.H. & EWING, R.C. (1976): The Harding mine, Taos County, New Mexico. *New Mexico Geol. Soc., 2th Field Conf., Guidebook*, 263-276.

JAMES, T.C. & MCKIE, D. (1958): The alteration of pyrochlore to columbite in carbonatites in Tanganyika. *Mineral. Mag.* **31**, 889-900.

JOHAN, V., MONIER, G. & ROSSI, P. (1988): Étude pétrographique systématique du granite du sondage GPF 1 de Beauvoir (complexe granitique d'Échassières, Massif Central français). *Bur. Rech. Géol. Min., Mém.* **124**, 11-101.

KNUDSEN, C. (1989): Pyrochlore group minerals from the Qaqarssuk carbonatite complex. *In* Lanthanides, Tantalum and Niobium (P. Möller, P. Černý & F. Saupé, eds.). Springer-Verlag, Berlin (80-99).

KOSAKEVITCH, A. (1976): Évolution de la minéralisation en Li, Ta et Nb dans la coupole granitique de Beauvoir (massif d'Echassières, Allier). *Bur. Rech. Géol. Min., Rapp.* **76** SGN 316 MGA.

KRIVOKONEVA, G.K. & SIDORENKO, G.A. (1971): The essence of the metamict transformation in pyrochlores. *Geochem. Int.* **8**, 113-122.

LACROIX, A. (1896): *Minéralogie de la France et de ses colonies*. **II.** Baudry-Béranger, Paris.

LONDON, D. (1986): Magmatic–hydrothermal transition in the Tanco rare-element pegmatite: evidence from fluid inclusions and phase-equilibrium experiments. *Am. Mineral.* **71**, 376-395.

_____ (1987): Internal differentiation of rare-element pegmatites: effects of boron, phosphorus, and fluorine. *Geochim. Cosmochim. Acta* **51**, 403-420.

LUMPKIN, G.R., CHAKOUMAKOS, B.C. & EWING, R.C. (1986): Mineralogy and radiation effects of microlite from the Harding pegmatite, Taos County, New Mexico. *Am. Mineral.* **71**, 569-588.

_____ & EWING, R.C. (1988): Alpha-decay damage in minerals of the pyrochlore group. *Phys. Chem. Minerals* **16**, 2-20.

MANNING, D.A.C. (1981): The effect of fluorine on liquidus phase relationships in the system Qz–Ab–Or with excess H_2O at 1 kbar. *Contrib. Mineral. Petrol.* **76**, 206-215.

MONIER, G., CHAROY, B., CUNEY, M., OHNENSTETTER, D. & ROBERT, J.-L. (1987): Evolution spatiale et temporelle de la composition des micas du granite albitique à topaze–lépidolite de Beauvoir. *Géol. France* **2-3**, 179-188.

OHNENSTETTER, D. & PIANTONE, P. (1988) : Géochimie et évolutions des minéraux du groupe des columbo-tantalites et des minéraux du groupe du pyrochlore du sondage GPF 1 Echassières (Allier). *Bur. Rech. Géol. Min., Mém.* **124**, 113-163.

PICHAVANT, M., BOHER, M., STENGER, J.F., AÏSSA, M. & CHAROY, B. (1987): Relations de phase des granites de Beauvoir à 1 et 3 kbar en conditions de saturation en H_2O. *Géol. France* **2-3**, 77-86.

PYATENKO, Y.A. (1959): Some aspects of the chemical crystallography of the pyrochlore-group minerals. *J. Crystallogr. Acad. Sci. USSR* **4**, 184-186.

ROSSI, P., AUTRAN, A., AZENCOTT, C., BURNOL, L., CUNEY, M., JOHAN, V., KOSAKEVITCH, A., OHNENSTETTER, D., MONIER, G., PIANTONE, P., RAIMBAULT, L. & VIALLEFOND, L. (1987): Logs pétrographique et géochimique du granite de Beauvoir dans le sondage "Échassières I": minéralogie et géochimie comparées. *Géol. France* **2-3**, 111-135.

SITNIN, A.A. & BYKOVA, A.V. (1962): The first specimen of microlite from granite. *Dokl. Acad. Sci. USSR* **147**, 141-144.

SUBRAMANIAN, M.A., ARAVAMUDAN, G. & SUBBA RAO, G.V. (1983): Oxide pyrochlore – a review. *Prog. Solid State Chem.* **15**, 55-143.

TERMIER, P. (1902): Sur la néotantalite, espèce minérale nouvelle. *Bull. Soc. Fr. Minéral.* **23**, 34-38.

VAN DER VEEN, A.H. (1963): A study of pyrochlore. *Verhand. Konink. Nederl. Geol. Mijnbouw Genoot.* **22**.

VAN WAMBECKE, L. (1970): The alteration processes of the complex titano-niobo-tantalates and their consequences. *Neues Jahrb. Mineral. Abh.* **112**, 117-149.

VORMA, A. & SIIVOLA, J. (1967): Sukulaite – $Ta_2Sn_2O_7$ – and wodginite as inclusions in cassiterite in the granite pegmatite in Sukula, Tammela in SW Finland. *C.R. Soc. géol. Finlande* **39**, 173-187.

WEBSTER, J.D., HOLLOWAY, J.R. & HERVIG, R.L. (1987): Phase equilibria of a Be, U, and F-enriched vitrophyre from Spor Mountain, Utah. *Geochim. Cosmochim. Acta* **51**, 389-402.

WEIDNER, J.R. & MARTIN, R.F. (1987): Phase equilibria of a fluorine-rich leucogranite from the St. Austell pluton, Cornwall. *Geochim. Cosmochim. Acta* **51**, 1591-1597.

WISE, M.A. & ČERNÝ, P. (1990): Primary compositional range and alteration trends of microlite from the Yellowknife pegmatite field, Northwest Territories, Canada. *Mineral. Petrol.* **43**, 83-98.

WYLLIE, P.J. & TUTTLE, O.F. (1961): Experimental investigation of silicate systems containing two volatile components. II. The effects of NH_3 and HF, in addition to H_2O, on the melting temperatures of albite and granite. *Am. J. Sci.* **259**, 128-143.

_____ & _____ (1964): Experimental investigation of silicate systems containing two volatile components. III. The effects of SO_3, P_2O_5, HCl, and Li_2O, in addition to H_2O, on the melting temperatures of albite and granite. *Am. J. Sci.* **262**, 128-143.

Received December 18, 1989, revised manuscript accepted July 13, 1991.